Theoret. Chim. Acta (Berl.) 61, 559–579 (1982)

THEORETICA CHIMICA ACTA

Assignment of Electronic Transitions by Geometry Optimization

P. C. Mishra* and Karl Jug

Theoretische Chemie, Universität Hannover, Callinstrasse 3A, D-3000 Hannover 1, Federal Republic of Germany

Adiabatic excitation energies, excited state geometries, excited state charges, bond orders and dipole moments have been obtained for HCN, CO_2,H_2CO, HFCO, F_2CO, ethylene, trans-butadiene, furan, pyrrole and uracil using the SINDO1 semi-empirical method with configuration interaction. Our results generally agree with those of *ab initio* calculations and experiment satisfactorily. Geometry optimization is found to mix configurations differing in their allowedness in vertical excitation from the ground state, which in turn helps in the assignment of spectral transitions. The *V* excited singlet state of trans-butadiene and various excited states of furan, pyrrole and uracil have been found to be appreciably non-planar. The single and double CC bonds are found to exchange positions due to the lowest triplet and singlet transitions of furan and pyrrole. The first triplet and first singlet transitions of uracil have been found to be of $\pi-\pi^*$ and $\pi-\sigma^*$ types respectively in agreement with recent experimental findings.

Key words: Assignment of electronic transitions – Excited state geometry optimization.

1. Introduction

Electronic excitation of a molecule is accompanied by a redistribution of charges and change of its geometry. A knowledge of these aspects is important for a proper assignment of spectral transitions and to understand molecular behaviour

---

* On leave of absence from the Department of Physics, Banaras Hindu University, Varanasi-221005, India

0040-5744/82/0061/0559/$04.20

in the excited state. In general, the degree of allowedness of forbiddenness of transitions in a molecule as obtained in a vertical excitation calculation would be modified following geometry optimization; this would be helpful in understanding the nature of the transitions better than what is possible from the vertical excitation calculation. Experimental study of excited state geometry is very difficult even for simple polyatomic molecules [1]. In the case of complex molecules, spectra are generally too diffuse to allow an analysis required for the excited state geometry determination. Therefore theory has to play an important role in this area.

Ab initio calculations on large molecules are expensive; this is why only vertical transitions have been studied for such systems [2–4]. Certain semi-empirical methods like CNDO/S-CI, INDO/CI are parameterized to yield good values of low lying singlet excitation energies in a vertical excitation calculation [5, 6], but they have several limitations. For example, they do not generally give satisfactory values of triplet excitation energies [7] and are not suitable for saturated systems. The SINDO1 method has been shown to reproduce ground state molecular geometries and properties satisfactorily [8, 9]; its applicability to excited states has been investigated in the present work. Another method which has a comparable scope as the present one and which has recently been applied to both ground and excited sates of certain molecules is MNDOC [10, 11].

2. Method of Calculations

Details of the SINDO1 method are available elsewhere [8, 9]. We have used this method in conjunction with configuration interaction (CI) treatment for the excited state calculations. The minimum value of ground state total energy was obtained using CI involving several singly and doubly excited configurations. Excitation energy was obtained as a difference of total energies of the optimized excited state and the ground state. The excited state hypersurface was generated by an SCF calculation for the ground state followed by a CI with a few necessary singly excited configurations of the valence shell. We usually started with vertical excitation from the ground state equilibrium. Geometry optimization was carried out by an approach based on the Newton–Raphson method [12] as described elsewhere [8]. All singly excited configurations which contributed significantly to excited state wavefunctions were used in the calculations except for uracil where CI of maximum 9×9 was used.

The symmetry of a molecule should be allowed to change without any restriction in the process of excited state geometry optimization. To judge the excited state symmetry, one would need to compare energies of the various possible symmetric and unsymmetric accurately optimized excited state geometries. This question was relevant in our work especially with regard to trans-butadiene, furan and pyrrole. Limiting our emphasis to the assignment of electronic transitions, we permitted symmetry reduction following excitations of these molecules as described below; it allows mixing of configurations that do not mix in the ground state molecular symmetry. We believe the various possible ways of symmetry reduction would lead to the same qualitative information on the nature of molecular transitions.

In trans-butadiene, an axis of symmetry was maintained during the opimization process. In furan and pyrrole, we maintained C_s symmetry with the symmetry plane passing through the middle of the C_1C_2 bond (see Figs. 2 and 3) and the heteroatom. By correlation of molecular orbitals of the ground and excited state equilibrium geometries, one can find which types of configurations mix appreciably following geometry deformation; it helps in assigning transitions from the point of view of ground state molecular symmetry and also reveals information about their nature and extent of allowedness reliably. Bond orders were calculated using the definition of Jug [13].

3. Results and Discussion

We can divide the molecules studied into two groups: (i) Test cases: This set includes HCN, CO_2, H_2CO, HFCO, F_2CO and ethylene. For these molecules we have results from *ab initio* calculations as well as experimental measurements due to other workers. So a study of these molecules helps in testing the predictive capability of the method, (ii) Large molecules: In this group we have studied trans-butadiene, furan, pyrrole and uracil. We present the results for adiabatic excitation energies, excited state geometries and dipole moments in Tables 1, 2 and 3 and Figs. 1 to 4b.

3.1. Test Cases

3.1a. Adiabatic Excitation Energies. Our calculated results for the various molecules of this group agree with those obtained experimentally and from *ab initio* calculations satisfactorily [14–32], except for H_2CO where the disagreement is of about 1 eV. It should, however, be mentioned that our calculation gives vertical triplet and singlet $n-\pi^*$ excitation energies of H_2CO with respect to the SCF ground state, as obtained usually in SCF-CI calculations [5, 6], respectively as 2.79 and 3.31 eV; these values agree reasonably with experimental results [15] as well as the vertical excitation energies due to Buenker and Peyerimhoff from an *ab initio* calculation [19]. For HFCO, our calculated $n-\pi^*$ triplet adiabatic excitation energy is much smaller than the vertical one; the latter compares satisfactorily with the vertical excitation energy from an *ab initio* calculation due to Ha and Keller [21]. According to our calculation, the ground state and triplet $n-\pi^*$ excited state potential energy hypersurfaces of HFCO cross so that the triplet lies below the ground state in its equilibrium geometry. This crossing of the hypersurfaces would facilitate decomposition of the molecule in the triplet $n-\pi^*$ state, and in this sense our finding gets support from Klimek and Berry who have contemplated decomposition of HFCO in the triplet state [33]. Our calculated excitation energies of ethylene are quite satisfactory and we get the V and Z singlet states to lie quite close together as found in other calculations also [11, 25]

Table 1. Excitation energies (eV)

	Present Results		*Ab initio Calc.*‡			*Experiment**	
Molecule	State†	Exc. Ener.	State	Exc. Ener.	MNDOC	State	Exc. Ener.
HCN	$T_1, {}^3A'$	4.87	${}^3A'$	4.42^{a}			
	$S_1, {}^1A''$	6.50	${}^1A''$	6.48^{a}	5.77	${}^1A''(\tilde{A})$	6.48^{b}
CO_2	$T_1, {}^3B_2$	4.46	${}^3B_2$	3.7^{c}		${}^3B_2$	3.36^{d}
	$S_1, {}^1A_2$	5.44	${}^1A_2$	4.5^{c}			
	$S_2, {}^1B_2$	5.88	${}^1B_2$	5.8^{c}	4.54	${}^1B_2(\tilde{A})$	5.8^{e}
H_2CO	$T_1, {}^3A''$	4.07	${}^3A''$	3.14^{f}	2.47	${}^3A''(\tilde{a})$	3.12^{b}
		(2.79)**	${}^3A_2$	3.01^{g}			
	$S_1, {}^1A_2$	4.52	${}^1A_2$	4.24^{f}	2.76	${}^1A''(\tilde{A})$	3.50^{b}
		(3.31)**	${}^1A_2$	3.43^{g}			
HFCO	$T_1, {}^3A$	1.35					
		(4.86)**		5.17^{h}			
	$S_1, {}^1A$	5.01		5.58^{h}		${}^1A(\tilde{A})$	4.69^{j}
				5.22^{i}			
	$T_1, {}^3A''$	3.36					
	$S_1, {}^1A''$	5.73		6.04^{i}			5.26^{k}
C_2H_4§	$T_1, {}^3B_1(T)$	2.88	${}^3B_1$	2.79	2.05	${}^3B_1$	2.85^{m}
	$S_1, {}^1B_1(V)$	5.96	${}^1B_1$	6.22	4.34	${}^1B_1$	$5.6^{\mathrm{p,q}}$
	$S_2, {}^1A_1(Z)$	6.0	${}^1A_1$	6.14	4.17		
Transbutadiene	$T_1, {}^3B_u(T)$	3.4	${}^3B_u$	3.31^{r}		${}^3B_u(\tilde{a})$	3.22^{s}
	$S_1, {}^1A_u$	6.8	${}^1A_u(R)$	6.53^{r}		$R(\tilde{C})$	6.66^{t}
	$S_2, {}^1B_u(V)$	7.41	${}^1B_u$	7.67^{r}		${}^1B_u(\tilde{A})$	$5.71–6.29^{\mathrm{t}}$
Furan	$T_1, {}^3B_2$	2.93	${}^3B_2(V)$	4.06^{u}			3.99^{v}
							(3.3–4.9)
	$S_1, {}^1B_2$	5.70	${}^1A_1(V)$	6.90^{u}		${}^1B_2(\tilde{A})$	6.06^{v} *st*
	$S_2, {}^1B_1$	6.23				${}^1A_1(\tilde{B})$	6.44,
							6.61^{v} *wk*
	$S_3, {}^1B_2$	7.15				${}^1A_1(\tilde{C})$	7.42^{v} *wk*
	$S_4, {}^1A_1$	7.67	${}^1B_2(V)$	7.58^{u}		${}^1B_2$ or	7.82^{v} *st*
						${}^1A_1$	
	$S_5, {}^1A_1$	8.18				R	8.05^{v} *wk*

Pyrrole	T_1, ${}^3B_2$	2.43	${}^3B_2(V)$	4.42^{w}		4.21^{v} (3.6–5.0)
	S_1, ${}^1A_2$	4.66	${}^1A_2(R)$	5.22^{w}	${}^1A_1$	$5.22^{v,x}$ *wk*
	S_2, ${}^1B_1$	5.92	${}^1B_1(R)$	6.05^{w}	${}^1B_2(\tilde{A})$	5.89, 5.98^{v} *st*
	S_3, ${}^1B_1$	6.27	${}^1B_1(R, V)$	6.13^{w}	R	$6.2–6.5^{v}$ *wk*
	S_4, ${}^1B_2$	6.61	${}^1B_2(R)$	6.33^{w}		
	S_5, ${}^1A_1$	7.41	${}^1A_1(V)$	6.73^{w}	${}^1A_1(\tilde{B})$	6.8, 6.93^{v} *ms*
			${}^1B_2(V)$	7.70	${}^1B_2$ or ${}^1A_1(\tilde{C})$	7.26 7.86^{v} *st*
Uracil	T_1	3.26		2.14^{y}		3.4^{z}
	S_1	4.86		5.19^{y}		$4.8, 5.1^{aa,bb}$
	S_2	5.64		6.16^{y}		$5.68^{aa,bb}$
	S_3	6.16		6.45^{y}		$6.0, 6.1^{bb}$
	S_4	7.06		7.22^{y}		$6.6, 6.8^{bb}$

---

* In the experimental work on furan and pyrrole, the assignment given is uncertain. The Herzberg notations are the same as in Ref. [2, 3, 4, 15, 40]. For T_1 of each of furan and pyrrole, the ranges covered by the observed peaks are indicated. Observed relative intensities of peaks are also indicated for furan and pyrrole using *st* = strong, *ms* = medium strong and *wk* = weak. For HCN to C_2H_4, the excitation energies compared are (0, 0) bands whereas for trans-butadiene, furan, pyrrole and uracil, the excitation energies are observed as peaks in optical absorption or electron impact spectra.

† The same designations T_n and S_n which stand respectively for triplet and singlet of number n are used in the figures and other tables.

‡ R stands for a Rydberg transition and V for one of valence type. For uracil, CNDO/S-CI results from Ref. [7] are compared.

†† From Ref. [11].

** Vertical excitation energy.

§ Assignment given in the D_{2d} point group of excited state.

[a] Ref. [14]
[b] Ref. [15]
[c] Ref. [16]
[d] Ref. [17]
[e] Ref. [18]
[f] Ref. [20]
[g] Ref. [19]
[h] Ref. [21]
[i] Ref. [22]
[j] Ref. [23]
[k] Ref. [24]
[l] Ref. [25]
[m] Ref. [26]
[p] Ref. [27]
[q] Ref. [28]
[r] Ref. [2]
[s] Ref. [38]
[t] Ref. [39]
[u] Ref. [3]
[v] Ref. [40]
[w] Ref. [4]
[x] Ref. [41]
[y] Ref. [7]
[z] Ref. [44]
[aa] Ref. [42]
[bb] Ref. [45]

Table 2. Excited state geometries of test cases (Å and Degrees)

Molecule	State	Coordinate	Present Results[a]	MNDOC[b]	Expt.	*Ab initio* Calc.
HCN	$T_1, {}^3A'$	CN	1.227			1.294[d]
		CH	1.079			1.081[d]
		HCN	120.4			128.6[d]
	$S_1, {}^1A''$	CN	1.244	1.294	1.297[c]	1.318[d]
		CH	1.09	1.125	1.140[c]	1.096[d]
		HCN	126.7	132.0	125.0[c]	127.2[d]
CO_2	$T_1, {}^3B_2$	CO	1.224			
		OCO	125.5			
	$S_1, {}^1A_2$	CO	1.223			
		OCO	138.0			
	$S_2, {}^1B_2$	CO	1.217	1.239	1.246[c]	
		OCO	136.0	133.9	122.0[c]	
H_2CO	$T_1, {}^3A''$	CO	1.246	1.279	1.307[e]	1.340[f]
		CH	1.068	1.111	1.096[e]	1.078[f]
		HCH	119.3	113.3	118.0[e]	119.7[f]
		OCH	117.3			
		OCH_2	27.5	32.8	37.9[e]	38.5[f]
	$S_1, {}^1A_2$	CO	1.245	1.290	1.325[e]	1.361[g]
		CH	1.066	1.102	1.095[e]	1.077[g]
		HCH	120.8	114.8	118.0[e]	120.0[g]
		OCH	119.6			
		OCH_2	0.0	26.0	33.6[e]	38.0[g]
HFCO	$T_1, {}^3A$	CO	1.365			
		CH	1.036			
		CF	1.313			
		OCF	111.7			
		OCHF	54.0			
	$S_1, {}^1A$	CO	1.262			
		CH	1.072			
		CF	1.329			
		OCF	120.6			
		OCHF	23.4			
F_2CO	$T_1, {}^3A''$	CO	1.363			
		CF	1.321			
		OCF	111.1			
		OCF_2	56.9			
	$S_1, {}^1A''$	CO	1.284			
		CF	1.324			
		OCF	114.0			
		OCF_2	43.3			
C_2H_4	$T_1, {}^3B_1$	CC	1.434	1.423	1.49[h]; 1.48[i]	
		CH	1.065	1.09	(1.076)[h]	
		HCH	120.0	116.5		(116.6)[h]
		HCCH	87.2			
	$S_1, {}^1B_1$	CC	1.310	1.338		1.40[h]; 1.43[i]
		CH	1.085	1.106		(1.076)[h]
		HCH	110.0	109.1		(116.6)[h]
		HCCH	91.8			

Table 2. (cont.)

Molecule	State	Coordinate	Present Results[a]	MNDOC[b]	Expt.	*Ab initio* Calc.
	S_2, $^1A_1$	CC	1.303	1.339		1.40[h]; 1.41[i]
		CH	1.083	1.107		(1.076)[h]
		HCH	111.8	108.8		(116.6)[h]
		HCCH	91.8			

[a] Ground state values are aviilable in Ref. [9]

[b] Ref. [11] [c] Ref. [15] [d] Ref. [14]

[e] Ref. [31] [f] Ref. [20] [g] Ref. [30]

[h] Ref. [32] Values given in parentheses were assumed.

[i] Ref. [25]

Table 3. Excited state dipole moments (Debye)

Molecule				State*			
	S_0	T_1	S_1	S_2	S_3	S_4	S_5
HCN	2.33	1.20	1.01				
CO_2	0.0	0.28	0.42	0.23			
H_2CO	1.48†	1.07†	0.83†				
	(2.33)	(1.29)	(1.56)				
HFCO	1.61	0.91	1.34**				
	(2.02)						
F_2CO	0.63	0.30	1.63				
Ethylene	0.0	0.0	0.0	0.0			
Trans-butadiene	0.0	0.0	0.0	0.54			
Furan	0.48	1.79	2.63	2.84	1.43	2.92	1.11
Pyrrole	1.75	2.30	1.80	3.72	3.24	0.84	1.98
Uracil	3.22	1.61	1.82	2.66	3.13	5.41	
	(3.9)§		(1.8)††				

* The ground state values of dipole moment, except that of uracil, have been taken from Ref. [9], where these are also compared with experimental results. Excited state values from experiment are given in parentheses and are available in Ref. [19, 36, 37, 50].

† *Ab initio* values from Ref. [19] for S_0, T_1 and S_1 respectively are 2.95, 1.88 and 1.68 Debye.

** Experimental value is uncertain, 1.93 or 3.0 Debye. See Ref. [36, 37].

§ See Ref. [50].

†† Observed change of dipole moment due to excitation, see Ref. [50].

3.1b. Excited State Geometries. These results for the test molecules are presented in Table 2. The corresponding ground state geometries are available in the literature [9]. Following the $^3A'$ and $^1A''$ transitions, HCN gets bent and the CN bond is elongated considerably according to our calculation, and it is in agreement with the findings from experiment and *ab initio* calculations [14, 15]. A similar situation occurs in CO_2 also. According to our calculation, formaldehyde becomes appreciably non-planar following the triplet $n-\pi^*$ transition and the CO bond length is increased. Consequent to the singlet $n-\pi^*$ transition, bond length and bond angle changes in H_2CO take place generally in the same way as due to the triplet $n-\pi^*$ transition, but our calculation predicts the singlet $n-\pi^*$ excited state geometry to be planar. It is not in agreement with experiment and other calculations [15, 19, 29–31]; however, it is not surprising as it is established [19, 29] that the potential energy hypersurface of the singlet $n-\pi^*$ excited state of H_2CO is very flat. The excited state energy changes in our calculation only by 0.1 k cal/mol when the molecule is made non-planar by 8°. Our calculations show that HFCO and F_2CO are also appreciably non-planar and the CO bond lengths are strongly increased in the triplet and singlet $n-\pi^*$ states. There are no earlier results on the excited state geometries of these molecules available for comparison.

Following the triplet and singlet transitions studied by us, ethylene becomes orthogonal from planar in the ground state. The CC bond length is considerably increased in the triplet state whereas it is somewhat decreased in the singlet states V and Z. In the MNDOC calculation of Schweig and Thiel [11] also the CC bond length is found to increase due to the triplet excitation, but no change occurs in this bond length due to the singlet excitations. *Ab initio* calculations [25] have shown that CC bond length is elongated in the V and Z excited states of ethylene also but by much smaller amounts than in the triplet state. It is also established [34, 35] that the singlet V state has an appreciable Rydberg character and therefore it is not surprising that both our calculation and that of Schweig and Thiel [11] which use only valence basis are unable to predict the CC bond length change in this excited state properly. According to our calculation the geometries of the excited states of ethylene are not exactly orthogonal; instead, the angles between the two CH_2 fragments differ by 2 to 3 degrees from 90°. In the calculations due to Schweig and Thiel [11], this angle was not perhaps fully optimized. At any rate, the surface is very flat at 90° and the energy difference between the exactly orthogonal and optimized geometries is less than 0.1 k cal/mol according to our calculation.

3.1c. Charges, Bond Orders, and Dipole Moments. The calculated charges and bond orders are not being presented but their features would be briefly discussed. The calculated dipole moments of all the molecules studied are presented in Table 3 and compared with the available *ab initio* and experimental results. We find that both the excitations T_1 and S_1 of HCN change the CN triple bond to a double bond and cause gain of electronic charges by the hydrogen atom; in T_1 the main loser of the charge is the carbon atom whereas in S_1 the main loser is the nitrogen atom. The dipole moment of HCN is reduced by more than 1 Debye due to both the excitations T_1 and S_1. In CO_2, the CO bond maintains its double bond character to a large extent, electronic charge migrates from oxygen to carbon and small dipole moments are generated due to all the three transitions studied. The triplet and singlet $n-\pi^*$ transitions of H_2CO, HFCO and F_2CO lead to concentration of elecronic charges on carbon at the cost of those at the other atoms including fluorine.

This is an interesting feature that despite the high electronegativity of fluorine, it does not attract electronic charges following the transitions. The reason is that in these molecules the n orbitals are mostly localized on oxygen and very little on carbon whereas the reverse is true for the π^* orbitals. Further, the n orbital in HFCO and F_2CO is localized on fluorine more than the π^* orbital. Consequently, the $n-\pi^*$ transitions in the molecules lead to migration of electronic charges mainly from oxygen but also to some extent from the other atoms towards carbon. The CO bond orders are reduced due to the $n-\pi^*$ transitions as expected. The net charges show that there is a complex interplay of bond moments in H_2CO, HFCO and F_2CO and mostly these moments are reversed in direction by the transitions. Consequently, though the dipole moments of the molecules are changed by the $n-\pi^*$ transitions, these changes in the various cases do not follow any regularity. According to the *ab initio* calculation of Buenker and Peyerimhoff and experiment, the dipole moment of H_2CO decreases following excitation [19, 36]; this is in agreement with our results.

The $n-\pi^*$ singlet excited state dipole moment of HFCO has been determined experimentally, but the results obtained are ambiguous [36, 37]. According to one value (1.93 Debye), the dipole moment would decrease slightly with respect to the ground state value (2.02 Debye), while according to the other (3 Debye), it would increase. Our calculation predicts that the dipole moment of HFCO would decrease by 0.27 Debye following the singlet $n-\pi^*$ excitation. The calculation of Ha and Keller [21] also predicts a decrease in the dipole moment of HFCO following its singlet $n-\pi^*$ transition by 0.43 Debye. In the experimental work, the smaller value has been prefered over the larger one; this choice is established to be correct by theory. Following the three transitions of ethylene, the CC bond order is reduced; this reduction is appreciable only in the triplet state. We found that our calculation does not properly describe the change of the CC bond length following the V singlet transition of ethylene, but it is interesting that bond orders do indicate a change in the appropriate direction.

3.2. *Larger Molecules*

3.2a. Adiabatic Excitation Energies. Our calculation reproduces the ^3B_u excitation energy of trans-butadiene [38] satisfactorily (see Table 1). The first singlet excitation energy of the molecule as well as the symmetry obtained by us agree with those due to Buenker et al. [2] from an *ab initio* calculation and also with those from experiment [39], but in both the latter studies [2, 9] the transition has been assigned as one of Rydberg type. The origin of the observed band corresponding to the ^1B_u (V) transition has not been exactly located [39] but it is known to lie between 5.71 and 6.29 eV. The ^1B_u transition energies obtained by us as well as by Buenker et al. [2] are appreciably larger than the experimental value [39] though in our calculation the agreement is somewhat improved.

In the following assignments for furan and pyrrole, we used the labels A_1, A_2, B_1, B_2 of the C_{2v} point group since the distortion to C_s correlates A_1 and B_1 to A' and A_2 and B_2 to A''. Our calculation agrees with the *ab initio* calculation of Thunemann et al. [3] and Butscher and Thunemann [4] respectively for furan and pyrrole in assigning the first triplets in these molecules as $^3B_2$. The experimentally observed peaks for the triplets of furan and pyrrole cover wide ranges and therefore the error in our calculted excitation energies cannot be estimated; however, our calculated triplet excitation energies are appreciably smaller than those suggested experimentally [40]. The first singlets of both furan and pyrrole arise from excitations from the highest occupied molecular orbital (HOMO) to the lowest unoccupied one (LUMO). In both these molecules, the HOMO is of a_2 type. The LUMO is of b_1 type in both the ground and excited state equilibrium geometries of furan, but it is a a_1 type in pyrrole in its ground state equilibrium geometry and maintains mainly this character even in the equilibrium geometry of the excited singlet though in the latter case it acquires a little b_1 character also. Therefore, the first excited singlet state of furan must be assigned as $^1B_2$ whereas that of pyrrole must be assigned as $^1A_2$. Thus the first excited singlet transition of pyrrole is found to have a strongly forbidden character as suggested by Mullen and Orloff [41]; it gets weakly allowed by geometrical deformations of the molecule. The assignment of Thunemann et al. [3] for the first singlet excited state of furan does not agree with ours as well as with that suggested in the experimental work [40]. Our assignment and that of Butscher and Thunemann [4] agree on the symmetry of the first excited singlet state of pyrrole as one of $^1A_2$ type, but according to these other authors the band has Rydberg nature. Two weak bands are observed in furan at 6.44 and 6.61 eV [40]. We may assume these two bands as components of the same electronic transition. According to our calculation, the electronic transition is of $^1B_1$ type. This assignment gets support from the observed weak intensity of the bands. Our calculation predicts a $^1B_2$ type of transition at 7.15 eV in furan. This is also, like the first singlet, largely composed of the HOMO→LUMO excitation. This calculated transition energy may be correlated with the band observed at 7.42 eV though this assignment does not immediately explain why the observed intensity of the band is weak. It is possible that the band is not weak, instead it could not be resolved from the next overlapping strong band. Another possibility is that the potential energy hypersurface of S_1 and S_3, which come fairly close to each other in the equilibrium geometry of S_3 (the separation there being only 0.76 eV according to our calculation), avoid their crossing thereby giving rise to a secondary minimum on the S_1 hypersurface. A transition from the ground state to this secondary minimum may be responsible for the weak band observed at 7.42 eV.

The fourth singlet transition in furan is obtained at 7.67 eV in our calculation. The occupied orbital mainly involved in this transition is of b_1 type in both the ground state and S_4 excited state equilibrium geometries. The virtual orbital mainly responsible for the transition is of b_1 type in the ground state, it maintains a strong b_1 character in the equilibrium geometry of S_4 also, but in the latter geometry it acquires some a_1 character. Therefore, the transition S_4 of furan should be assigned as $^1A_1$. The corresponding band observed at 7.82 eV is strong and has been ambiguously assigned as $^1B_2$ or $^1A_1$ in the experimental work [40]. Thunemann et al. assign it as one of $^1B_2$ type from their *ab initio* calculation of vertical excitations [3]. The band observed experimentally at 8.05 eV has a weak intensity and has been tentatively assigned as one of Rydberg type [40]. We correlate it with our calculated transition energy at 8.18 eV. In our calculation, the excited state wave function in the equilibrium of S_5 has two main components; the larger one arises from an $a_2 \rightarrow a_2$ orbital excitation whereas the other somewhat smaller one arises from a $b_1 \rightarrow a_1$ orbital excitation. We assign the transition as one of $^1A_1$ type on the basis of the larger component. But as the transition has an appreciable amount of B_1 character, we do not expect it to appear as a strong band which agrees with experimental observations [40]. A vertical excitation calculation cannot yield this information since configurations which belong to A_1 and B_1 representations in the C_{2v} point group cannot mix. It shows how excited state geometry optimization may be helpful in understanding the nature of electronic transitions.

The second observed band in the spectrum of pyrrole lies at about 5.9 eV [40]. Butscher and Thunemann [4] assign this band to a B_1 (Rydberg) transition. Our calculation also yields a B_1 type of singlet transition at 5.92 eV which we correlate with this observed band. Even though our calculation and that due to Butscher and Thunemann [4] agree on assigning the band to a $^1B_1$ transition, it is not clear why it appears with a strong intensity though the following explanation may be given on the basis of our calculations.

The sequence a_1, b_1, b_2 of unoccupied orbitals in the ground state is reversed to b_1, b_2, a_1 in S_2. The crossing is due to the partial occupation of the b_1 and b_2 orbitals in this excited state whereas the a_1 orbital remains unoccupied. Therefore, it is likely that the B_1 type of transition which arises from an $a_2 \rightarrow b_2$ excitation in the equilibrium geometry of the excited singlet is overlapped in the observed spectrum by a vertical transition from the ground state, the corresponding excitation being from the HOMO(a_2) to the orbital next to LUMO(b_1); it may be responsible for the strong overall appearance of the band. We found the above mentioned vertical excitation energy to be 6.67 eV which compares with the energy of the observed peak within the expected deviation.

A few weak bands are observed in the spectrum of pyrrole in the range 6.2 to 6.5 eV [40]. In the experimental work, these are assigned as Rydberg transitions [40]. Butscher and Thunemann [4] correlate their calculated vertical transition energies 6.13 and 6.33 eV, one corresponding to a mixed (Rydberg + valence) type of transition and the other to a purely Rydberg transition with these bands. The singlet transition energy obtained by us at 6.27 eV may also be correlated to a band in this region. It arises in our calculation mainly from an $a_2 \rightarrow b_2$ orbital excitation which is in agreement with the observed weak intensity of the band.

Our calculation yields a transition energy of 6.61 eV corresponding to a $^1B_2$ excited state. This transition is composed of two main parts, the larger one arises from the HOMO(a_2)$\rightarrow$LUMO(b_1) excitation on the basis of which we have made the assignment, and the other somewhat smaller one which involves the orbital excitation $a_2 \rightarrow a_1$. This mixing would not occur in a vertical excitation calculation. Therefore, because of its substantially forbidden nature, the calculated transition at 6.61 eV may be correlated with one of the weak bands observed in the region 6.2 to 6.5 eV. The nature of this transition of pyrrole resembles that calculated at 7.15 eV for furan in the sense that both these are mainly composed of HOMO→LUMO excitation, like S_1. Therefore, the explanation we gave for the weak observed band at 7.42 eV in furan in terms of a secondary minimum on the S_1 hypersurface is also likely to be valid for this transition in pyrrole.

The fifth singlet transition energy of pyrrole is obtained in our calculation at 7.41 eV, the excited state being of A_1 type. The corresponding observed band has a medium strong intensity and has also been assigned both by Flicker et al. [40] and by Butscher and Thunemann [4] as one of A_1 type. Our calculated fifth singlet transition energy might also be correlated with the strong broad band observed in the region 7.26 to 7.86 eV.

We observe a parallelism between our results and those due to Butscher and Thunemann for pyrrole [4]. That is, corresponding to each Rydberg transition obtained by these authors, we have a forbidden or appreciably forbidden type of transition arising from excitations between π and σ valence orbitals. A comparison of our calculated first singlet transition of trans-butadiene with the corresponding result from the *ab initio* calculation of Buenker et al. [2] shows the same situation. These observations seem to suggest that a good representation of the transitions may be obtained by using a basis set consisting of both valence and Rydberg orbitals.

Uracil is a molecule of great photobiological significance. Though numerous vertical excitation calculations and experimental studies have been carried out on its spectrum [7], yet knowledge about the nature of its excited states is very vague [42]. In our calculation, we have included possible non-planarity in its excited state geometry which makes the molecule highly unsymmetric in the excited states. In the ground state of uracil, the HOMO is of π type; it continues to be dominantly so in the various excited state geometries. The occupied orbital just below HOMO is of σ type with about 45% localization on O_8 (see Fig. 4a) and so it may be approximately designated as one of non-bonding(n) type. The LUMO is of σ^* type in the ground state whereas the next higher orbital is of π^* type; both these orbitals have mixed $(\sigma + \pi)$ characters in the different excited state equilibrium geometries. The photoelectron spectrum of uracil has been studied experimentally [43]. In this work it has been shown that the first five ionization potentials of uracil are 9.6, 10.15, 10.6, 11.2 and 12.63 eV [43]. They have respectively been assigned to removal of π, $\sigma(n)$, π, $\sigma(n)$, and π electrons from the molecule. Our calculation in the Koopmans' approximation gives quite satisfactory values of the ionization potentials: 9.4, 10.0, 10.5, 10.7 and 13.6 eV with identically the same assignment as found in the experimental work [43].

The first triplet vertical transition energy of uracil from the ground state is of $\pi - \pi^*$ type corresponding to an excitation from the HOMO to the orbital next to LUMO, but the transition is found to be dominated by the HOMO to LUMO excitation on geometry optimization; however, the excitation that is responsible for the vertical transition also contributes significantly in its equilibrium geometry. Because of a major π-character of LUMO in the equilibrium geometry of the triplet, the transition may be classified as one of $\pi-\pi^*$ type in agreement with experiment [42–44].

Our calculated first singlet transition energy of uracil is in a good agreement with the experimental value [45]. We found the lowest singlet vertical transition from the ground state to arise from the HOMO(π) to LUMO(σ^*) excitation. The lowest vertical singlet $\pi-\pi^*$ transition energy (from HOMO to next to LUMO) lies about 1 eV higher than this singlet. Even in the optimized geometry of the first excited singlet state, a dominant contribution comes from the HOMO to LUMO excitation; however, due to geometrical deformations, the LUMO acquires an appreciable π-character in this case. Thus the transition may be assigned as one of $\pi-\sigma^*$ type. Consequently, it is expected to have a forbidden character getting partly allowed due to geometrical deformations. Our finding gets support from a recent experimental study [42] where the first singlet transition of a related molecule thymine has been found to have an appreciably forbidden character, since the same is likely to be qualitatively true for uracil also.

Transition energies for all the three higher singlet excited states of uracil S_2, S_3 and S_4 are also obtained satisfactorily by our calculations. These transitions are mainly composed of $\pi-\pi^*$ and $\sigma(n)-\sigma^*$ excitations. Presence of $n-\pi^*$ transitions has been conjectured in the spectrum of uracil and in particular the 5.88 eV transition is believed to be one of this type [42]. We got a singlet transition of $n-\pi^*$ type at 7.36 eV in our vertical excitation calculation but none of the excited states S_2, S_3 or S_4 shows this character clearly in its equilibrium. All these three transitions get appreciable contributions in the excited state equilibrium geometries from excitations from the n orbital, 26%, 22% and 78% respectively where both $n-\pi^*$ and $n-\sigma^*$ contributions have been added. In S_4, a major contribution comes from a $n-\sigma^*$ excitation and only a minor part comes from a $n-\pi^*$ excitation. Thus because of appreciable contributions from excitations from the n-orbital, these transitions may show behaviour similar to that of a $n-\pi^*$ transition (e.g. blue shift on increasing solvent polarity). But our results suggest that none of the transitions should really be assigned as $n-\pi^*$.

3.2b. Excited State Geometries. Ground state geometries of trans-butadiene, furan and pyrrole as calculated by the SINDO1 method are available elsewhere [9]. The present calculated excited state geometries of trans-butadiene are given in Fig. 1. We find that the C_1C_2 bond length is elongated while the C_2C_3 bond length is shortened following all the three transitions studied, but these changes are most pronounced in T_1. Changes of bond angles following the three transitions are also appreciable, but the most pronounced changes in bond angles occur in S_1, T_1 and S_1, like the ground state, are planar but S_2 is considerably non-planar.

The excited state geometries of furan and pyrrole are presented in Figs. 2 and 3 respectively. These molecules are found to be more or less non-planar in all of their excited states studied. We find that the equivalent hydrogen atoms (6 and 7 or 8 and 9) are always displaced on the same side of the plane of carbons. Further, the non-equivalent hydrogen atoms lying on the same side of the molecule (6 and 9 or 7 and 8) may be on the same side or on opposite sides of

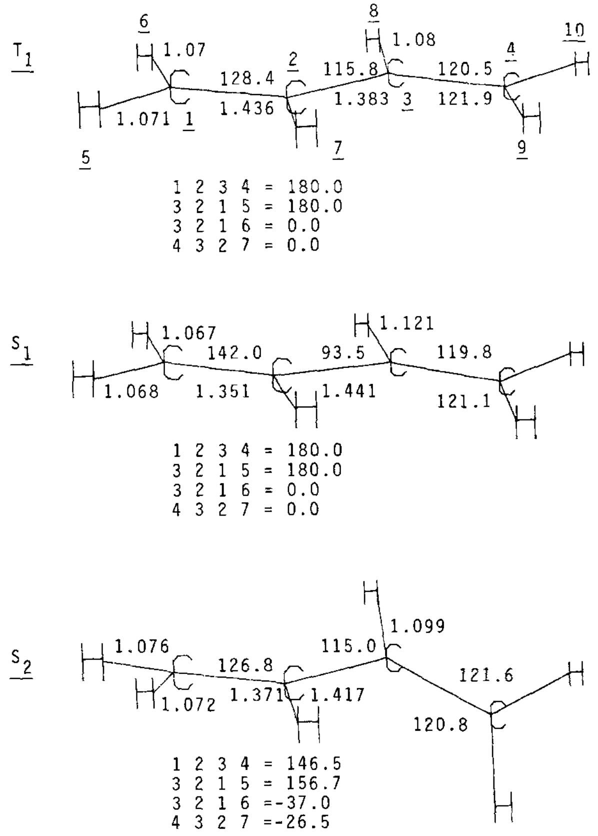

Fig. 1. Geometries of different excited states of trans-butadiene (Å and Degrees). The underlined numbers represent the atomic numbering scheme used

the plane of carbons. Thus ignoring oxygen in furan and NH group in pyrrole, we get in general two types of excited state geometries for these molecules. One of these is of chair type (type 1) while the other is of boat type (type 2). Using this description, the first triplet and first five singlets of furan have geometries of the types 1, 2, 1, 1, 2, and 1 respectively. In pyrrole, the corresponding geometries are of types 1, 1, 1, 2, 2 and 2 respectively.

In going from S_0 to T_1 and S_1 of furan, the positions of the single and double CC bonds are reversed; this is pronounced particulary in T_1. It implies that in each of T_1 and S_1 of furan on the whole one double bond is missing compared to the ground state; these excited states may therefore be classified as of biradicaloid type [46]. In S_2 and S_3 of furan, the CC bond lengths tend to be equal whereas the transitions S_4 and S_5 lead to elongation of all the CC bonds so that the C_1C_2 bond is appreciately longer than the C_2C_3 bond as in the ground state. In all the excited states of furan, the CO bond lengths are somewhat shorter than the ground state value. In T_1 and S_1 of pyrrole, we observe the same type of bond reversal as we get in furan. In S_2, S_3, S_4 and S_5 of pyrrole,

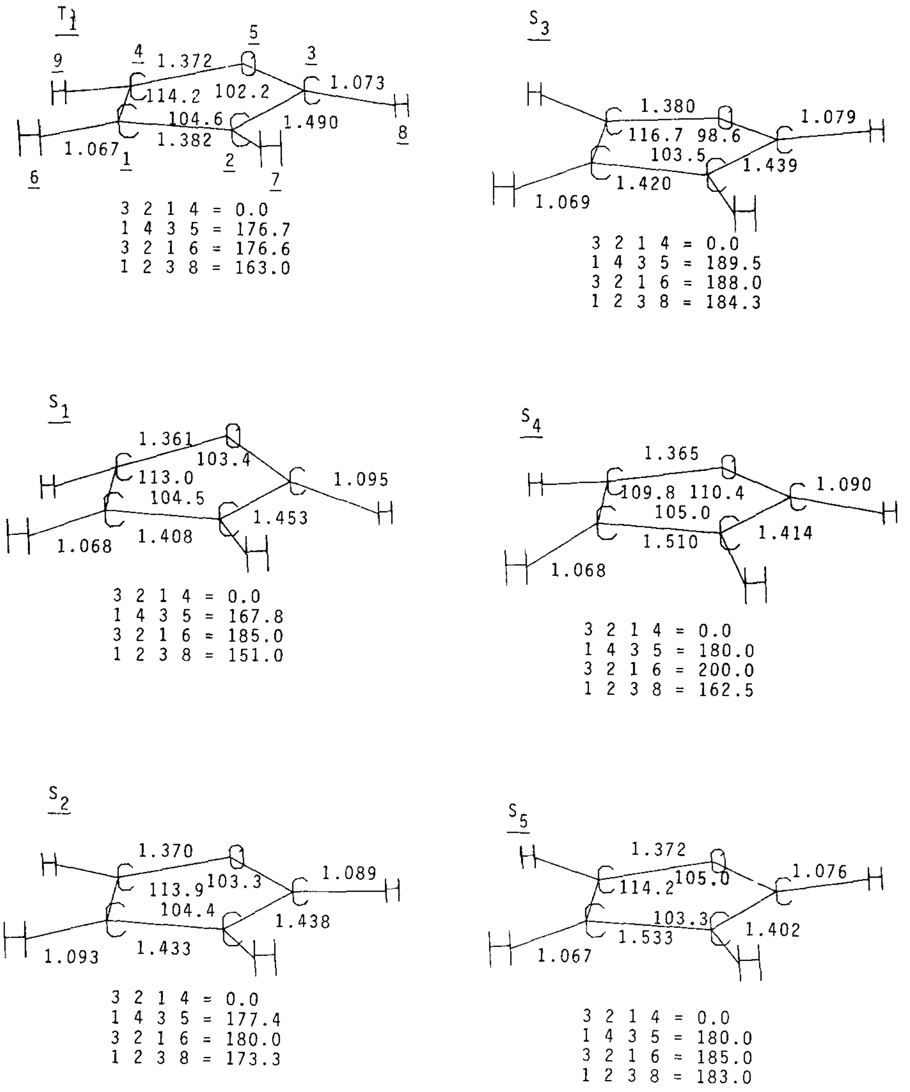

Fig. 2. Geometries of different excited states of furan (Å and Degrees). The underlined numbers represent the atomic numbering scheme used

the C_1C_2 bond is larger than the C_2C_3 bond as in the ground state, but the differences are much smaller in the excited states. Except in S_1, the CN bond length changes due to the transitions in pyrrole are small.

The ground state geometry of uracil obtained in the present work is shown in Fig. 4a. A comparison of this geometry with that due to Zielinski et al. [47] from an *ab initio* calculation and Voet and Rich from experiment [48] shows that the error in our calculation is generally of the same order as in the *ab initio* calculation [47]. Excited state geometries of uracil are presented in Figs. 4a and

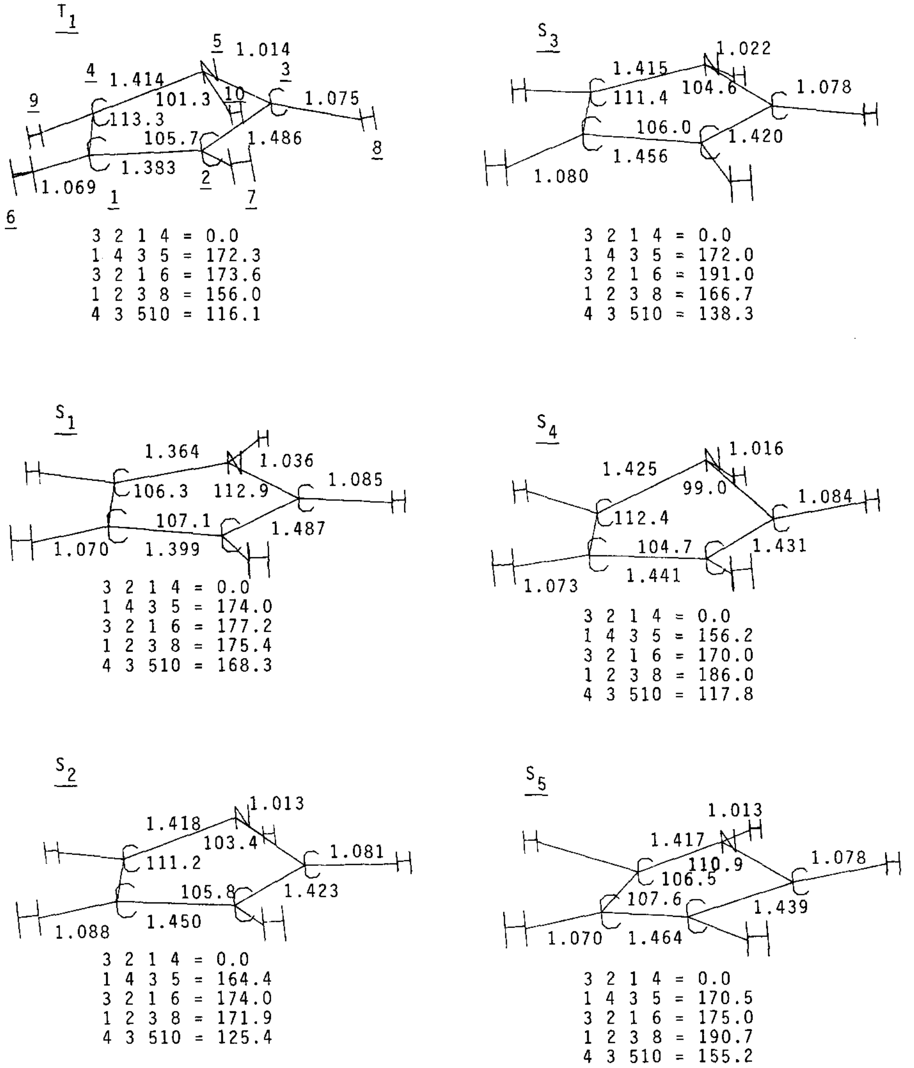

Fig. 3. Geometries of different excited states of pyrrole (Å and Degrees). The underlined numbers represent the atomic numbering scheme used

4b. We find that all the excited states of uracil are appreciably non-planar. It is expected to have important effects on the photophysical properties of the molecule [42]. The C_3C_4 bond length (usually numbered as C_5C_6) is considerably elongated due to all the transitions except S_2. The elongation of the C_3C_4 bond in T_1 is so strong that the bond acquires a single bond character from a double bond in the ground state. The bond angles $C_2C_3C_4$ and $C_3C_4C_5$ are decreased following all the transitions and this decrease is also maximum in T_1. It seems worth mentioning that due to the transitions the atoms H_7 and O_{12} of uracil (*U*) which are involved in hydrogen bonding with adenine (*A*) in the *A*–*U* base pair in RNA generally get appreciably displaced below or above the rest of the ring. It would affect hydrogen bonding in the base pair.

3.2c. Charges, Bond Orders, and Dipole Moments. The CC bond orders for trans-butadiene show that the C_1C_2 and C_2C_3 bonds which are typically double

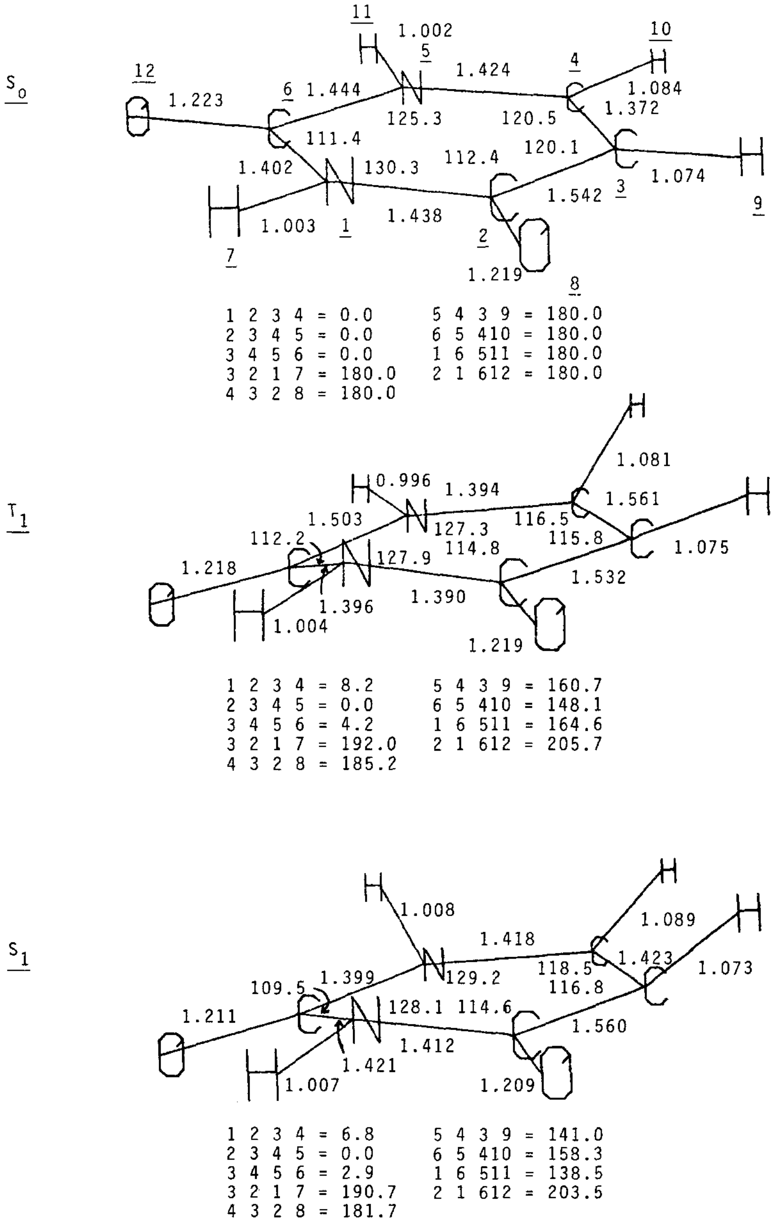

1 2 3 4 = 0.0
2 3 4 5 = 0.0
3 4 5 6 = 0.0
3 2 1 7 = 180.0
4 3 2 8 = 180.0
5 4 3 9 = 180.0
6 5 4 10 = 180.0
1 6 5 11 = 180.0
2 1 6 12 = 180.0

1 2 3 4 = 8.2
2 3 4 5 = 0.0
3 4 5 6 = 4.2
3 2 1 7 = 192.0
4 3 2 8 = 185.2
5 4 3 9 = 160.7
6 5 4 10 = 148.1
1 6 5 11 = 164.6
2 1 6 12 = 205.7

1 2 3 4 = 6.8
2 3 4 5 = 0.0
3 4 5 6 = 2.9
3 2 1 7 = 190.7
4 3 2 8 = 181.7
5 4 3 9 = 141.0
6 5 4 10 = 158.3
1 6 5 11 = 138.5
2 1 6 12 = 203.5

Fig. 4a. Geometries of the ground state, the first triplet and first singlet excited states of uracil (Å and Degrees). The underlined numbers represent the atomic numbering scheme used.

$\underline{S_2}$

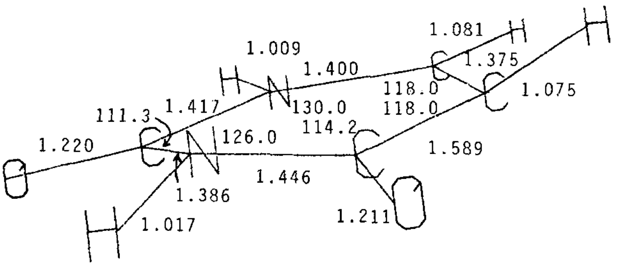

1 2 3 4 = 8.6
2 3 4 5 =-1.4
3 4 5 6 = 2.0
3 2 1 7 = 202.0
4 3 2 8 = 190.4

5 4 3 9 = 152.4
6 5 410 = 184.1
1 6 511 = 176.4
2 1 612 = 195.3

$\underline{S_3}$

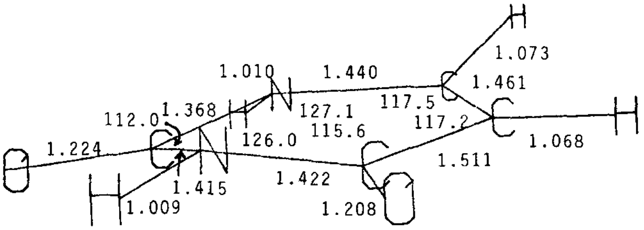

1 2 3 4 = 8.6
2 3 4 5 =-2.6
3 4 5 6 = 8.5
3 2 1 7 = 187.2
4 3 2 8 = 181.2

5 4 3 9 = 123.1
6 5 410 = 168.0
1 6 511 = 191.0
2 1 612 = 194.5

$\underline{S_4}$

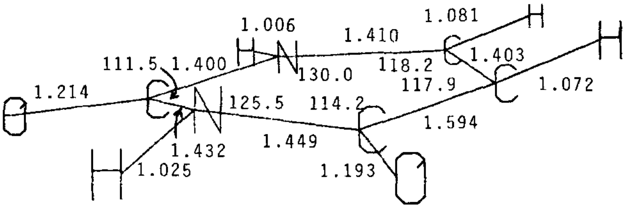

1 2 3 4 = 8.3
2 3 4 5 =-1.2
3 4 5 6 = 3.0
3 2 1 7 = 196.2
4 3 2 8 = 188.6

5 4 3 9 = 152.5
6 5 410 = 181.1
1 6 511 = 182.3
2 1 612 = 194.5

Fig. 4b. Geometries of the second, third and fourth excited singlet states of uracil (Å and Degrees). The underlined numbers represent the atomic numbering scheme used

and single CC bonds respectively in the ground state maintain this distinction to some extent in S_1; in T_1 and S_2 these bonds acquire intermediate character. T_1 and S_2 of trans-butadiene have similar charge distributions which are different from that in S_1. The molecule has an appreciable dipole moment in S_2 which arises from its non-planar geometry (see Table 3). The excited state bond orders of furan and pyrrole support the conclusion drawn earlier that the C_1C_2 and C_2C_3 bonds undergo reversal of their nature due to the transitions T_1 and S_1. The bond orders for the higher excited states of furan also confirm the conclusion drawn earlier that the CC bonds approximately maintain their ground state character in S_4 and S_5 whereas in S_2 and S_3 there is appreciable electron delocalization on the ring; the bond orders for the CC bonds are close to 1.5 in the latter two cases. Therefore, it appears that the excited states S_2 and S_3 of furan have appreciable aromatic character. The bond orders for the excited states S_2, S_3, S_4 and S_5 of pyrrole show that there is more electron delocalization in general on the ring in these cases than in the corresponding excited states of furan.

Our calculated net charges show that the CO and CN bonds in furan and pyrrole respectively have appreciably polar nature in the ground and various excited states. From the point of view of excited state ring geometries, charges and bond orders, the excited states T_1, S_1, S_2, S_3, S_4 and S_5 of pyrrole resemble respectively T_1, S_1, S_2, S_4, S_3 and S_5 of furan. It is interesting to note that the group theoretical representations of the excited states of the two molecules when compared in the above mentioned sequence also show some similarity. The difference is that while S_1 and S_4 in furan have B_2 and A_1 representations respectively, in pyrrole these states have the representations A_2 and B_1 respectively. This shows that the excited states of furan and pyrrole have a good deal of qualilative similarity but the relative weights of A_2 and B_2 or A_1 and B_1 representations may be different in their corresponding transitions. Consequently, though the gross physical appearances of spectra of the two molecules are also similar, intensities of the peaks generally have different origins.

The charges and bond orders for uracil show, like the geometries discussed earlier, that the various transitions of uracil have certain similarities. The C_3C_4 bond order decreases strongly in the excited triplet state. This would enhance free valences at C_3 and C_4 and facilitate the well known photodimerization reaction [49]. The C_3C_4 bond order in uracil is appreciably decreased in the first excited singlet state also, but by a considerably smaller amount; this correlates with the experimental observation that stable photodimers form generally in the excited triplet state [49] but the reaction takes place in the first excited singlet state also.

The calculated dipole moments for the ground and various excited states of furan, pyrrole and uracil are presented in Table 3. We find that excepting S_4 of pyrrole, dipole moments of furan and pyrrole are increased following excitation. It has been experimentally observed that the dipole moment of uracil changes by 1.8 Debye following the first singlet transition [50]. This value compares reasonably with the change 1.4 Debye calculated by us. However, in the experimental work [50], the change of dipole moment has been interpreted as increase, whereas the present calculation shows it to be a decrease. Since the evaluation of the experimental result is based on certain assumptions like the main contribution to dipole moment coming from the two carbonyl groups, which is not supported by our calculated net charges, the sign of the experimentally determined change of dipole moment may not be reliable.

Acknowledgement. One of the authors (P.C.M.) thanks the Alexander von Humboldt-Stiftung, Bonn for the award of a fellowship. The computations were performed with a CYBER 76 at the Universität Hannover.

References

1. Cvitaŝ, T., Hollas, J M., Kirby, G. H.: Mol. Phys. **19**, 305 (1970)
2. Buenker, R. J., Shih, S., Peyerimhoff, S. D.: Chem. Phys. Letters **44**, 385 (1976).
3. Thunemann, K.-H., Buenker, R. J., Butscher, W.: Chem. Phys. **47**, 313 (1980)
4. Butscher, W., Thunemann, K.-H.: Chem. Phys. Letters **57**, 224 (1978) (See also the references given therein)
5. DelBene, J., Jaffe, H. H.: J. Chem. Phys. **48**, 1807 (1968)
6. Ridley, J., Zerner, M.: Theoret. Chim. Acta **32**, 111 (1973)
7. Srivastava, S. K., Mishra, P. C.: Int. J. Quantum Chem. **18**, 827 (1980)
8. Nanda, D. N., Jug, K.: Theoret. Chim. Acta **57**, 95 (1980)
9. Jug, K., Nanda, D. N.: Theoret. Chim. Acta **57**, 107, 131 (1980)
10. Thiel, W.: J.Am. Chem. Soc. **103**, 1413, 1420 (1981)
11. Schweig, A., Thiel, W.: J. Am. Chem. Soc. **103**, 1425 (1981)
12. Himmelblau, D. M.: Applied nonlinear programming, New York: McGraw-Hill, 1972
13. Jug, K.: J. Am. Chem. Soc. **99**, 7800 (1977); Theoret. Chim. Acta **51**, 331 (1979)
14. Schwenzer, G. M., O'Niel, S. V., Schaefer, H. F., III, Baskin, C. P., Bender, C. F.: J. Chem. Phys. **60**, 2787 (1974)
15. Herzberg, G.: Electronic spectra of polyatomic molecules. New York: Van Nostrand Reinhold Co., 1966
16. Winter, N. W., Bender, C. F., Goddard, W. A.: Chem. Phys. Letters **20**, 489 (1973)
17. Mohammed, H. H., Fournier, J., Deson, J., Vermeil, C.: Chem. Phys. Letters **73**, 315 (1980)
18. Dixon, R. N.: Discuss. Farad. Soc. **35**, 105 (1963)
19. Buenker, R. J., Peyerimhoff, S. D.: J. Chem. Phys. **53**, 1368 (1970)
20. Adams, G. F., Bent, G. D., Bartlett, R. J., Purvis, G. D.: J. Chem. Phys. **75**, 834 (1981)
21. Ha, T.-K., Keller, L.: J. Mol. Struct. **27**, 225 (1975)
22. DelBene, J. E., Worth, G. T., Marchese, F. T., Conrad, M. E.: Theoret. Chim. Acta **36**, 195 (1975)
23. Fischer, G.: J. Mol. Spectry. 29, 37 (1969)
24. Workman, G. L., Duncan, A. B. F.: J. Chem. Phys. **52**, 3204 (1970)
25. Buenker, R. J., Peyerimhoff, S. D.: Chem. Phys. **9**, 75 (1976)
26. Douglas, J. E., Rabinovitch, B. S., Looney, F. S.: J. Chem. Phys. **32**, 2439 (1955)
27. McDiarmid, R.: J. Chem. Phys. **55**, 4669 (1971)
28. Mulliken, R. S.: J. Chem. Phys. **66**, 2448 (1977) (See also the references given therein)
29. Ha, T.-K.: J. Mol. Struct. **21**, 331 (1974)
30. Bell, S.: Mol. Phys. **37**, 225 (1979)
31. Jones, V. T., Coon, J. B.: J. Mol. Spectry. **31**, 137 (1969)
32. Brooks, B. R., Schaefer, H. F., III: J. Am. Chem. Soc. **101**, 307 (1979)
33. Klimek, D. E., Berry, M. J.: Chem. Phys. Letters **20**, 141 (1973)
34. McMurchie, L. E., Davidson, E. R.: J. Chem. Phys. **66**, 2959 (1977)
35. Buenker, R. J., Peyerimhoff, S. D., Shih, S.-K.: J. Chem. Phys. **69**, 3882 (1978)
36. Liptay, W.: Excited states, Vol. 1, P. 129 E. C. Lim (ed.), New York: Academic Press, 1974, (See also the references given therein)
37. Lombardi, J. R., Campbell, D., Klemperer, W.: J. Chem. Phys. **46**, 3482 (1967)
38. Mosher, O. A., Flicker, W. M., Kuppermann, A.: J. Chem. Phys. **59**, 6502 (1973)

39. McDiarmid, R.: J. Chem. Phys. **64**, 514 (1976)
40. Flicker, W. M., Mosher, O. A., Kuppermann, A.: J. Chem. Phys. **64**, 1315 (1976)
41. Mullen, P. A., Orloff, M. K.: J. Chem. Phys. **51**, 2276 (1969)
42. Becker, R. S., Kogan, G.: Photochem. Photobiol. **31**, 5 (1980)
43. Padva, A., O'Donnell, T. J., LeBreton, P. R.: Chem. Phys. Letters **41**, 278 (1976)
44. Salet, C., Benasson, R., Becker, R. S.: Photochem. Photobiol. **30**, 325 (1979)
45. Clark, L. B., Tinoco, I., Jr.: J. Am. Chem. Soc. **87**, 11 (1965)
46. Michl, J.: Excited states in quantum chemistry, Proceedings of the NATO Advanced Study Institute held at Kos, Greece, Nicolaides, C. A., Beck, D. R. (eds.), p. 417, Reidel Publishing Co. 1979
47. Zielinski, T. J., Shibata, M., Rein, R.: Int. J. Quantum Chem. **19**, 171 (1981)
48. Voet, D., Rich, A.: Prog. Nucl. Acid Res. Mol. Biol. **10**, 247 (1970)
49. Srivastava, S. K., Mishra, P. C.: Int. J. Quantum Chem. **16**, 1051 (1979)
50. Seibold, K., Labhart, H.: Biopolymers **10**, 2063 (1971)

Received March 22, 1982